# Computational aspects of concrete fracture simulations in the framework of the SDA

C. Feist & G. Hofstetter

*Institute for Structural Analysis and Strength of Materials, Innsbruck, Austria*

ABSTRACT: A numerical model within the framework of the nonsymmetric formulation of the strong discontinuity approach (SDA) for fracture simulations is investigated. Shortcomings of the basic formulations are analyzed and potential methods to overcome them are discussed. A new tracking algorithm intending to enforce continuity of the crack is proposed. The proposed model is applied to simulations of academic and large-scale problems.

Keywords: SDA, tracking algorithm, nonlocal averaging, dam

## 1 INTRODUCTION

The strong discontinuity approach (SDA) has gained wide popularity in FEM-based simulations of concrete fracture over the last years. In the SDA macroscopic cracking of quasi-brittle materials is represented by embedding a discontinuous displacement field in finite elements (Oliver 1996a). Thus, in contrast to the classical smeared crack approach it allows for a proper kinematic resolution of a macroscopic crack without the need for any regularization. On the other hand extensive remeshing – typically necessary for discrete crack-models – is avoided as cracks may cross FE-meshes in arbitrary ways. In its basic formulation the method exhibits a strictly local character. Despite of its conceptual simplicity it turned out that the SDA found in the original formulations implies some shortcomings which render it not fully objective. The major drawback can be found in its sensitivity with respect to the mesh-layout (Jirásek & Zimmermann 2001).

This paper addresses some computational aspects of a particular implementation within the SDA framework. It starts with the basic local formulation and shows its shortcomings. The necessary ingredients to overcome the deficiencies are applied step-by-step leading to an objective formulation.

The main features of the particular SDA-model presented in this work are effective algorithms for determining the direction of a propagating crack and for enforcing a continuous crack-path across finite elements.

It is shown that enforcing a continuous crack-path is a necessary ingredient for the particular formulation. It alleviates the pathology of mesh-sensitivity and resulting locking-effects, although the local character of the model is lost. Enforcement of continuous crack-paths is established by tracking algorithms (Oliver et al. 2003). Established algorithms are briefly outlined and a new strategy is proposed.

In classical models the determination of the crack-propagation direction relies on information derived from a suitable constitutive model. For instance, when applying the SDA to concrete fracture simulations the maximum principal stress direction may be chosen corresponding to a RANKINE criterion for mode-I fracture. However, principal stress directions derived from the local stress field more or less differ from realistic macroscopic crack directions. By employing a nonlocal averaging procedure macroscopic cracks are recovered objectively.

The capabilities of the model are demonstrated by its application to simulations of both laboratory tests and a large-scale dam analysis. The presented work is done in the framework of the thematic network *Integrity Assessment of Large Concrete Dams (NW-IALAD)* (Ialad 2003). The aim of the network is to conduct a state of the art review on integrity and safety assessment tools for concrete dams.

## 2 BASIC SDA MODEL

### 2.1 *The strong discontinuity kinematics*

Consider a two-dimensional domain $\Omega$ crossed by a fixed material (localization) line $\Gamma$, which is defined by its unit normal vector $\boldsymbol{n}$. It represents, for instance, a macroscopic crack in concrete. The localization line splits $\Omega$ into two portions $\Omega^+$ (pointed by $\boldsymbol{n}$) and $\Omega^-$ such that $\Omega^+ \cup \Omega^- = \Omega \setminus \Gamma$ (Oliver at al. 2003). Assuming the displacement field $\boldsymbol{u}(\boldsymbol{x})$ to exhibit a jump across the localization line an additive decomposition of the displacement field into a regular part $\bar{\boldsymbol{u}}$ and a term $\hat{\boldsymbol{u}}$ related to the displacement jump – i.e. the crack-opening – can be postulated:

$$
\begin{aligned}
\boldsymbol{u}(\boldsymbol{x}) &= \bar{\boldsymbol{u}}(\boldsymbol{x}) + \hat{\boldsymbol{u}}(\boldsymbol{x}), \quad \forall \boldsymbol{x} \in \Omega \\
\hat{\boldsymbol{u}} &= [\![\boldsymbol{u}]\!]\, M_\Gamma(\boldsymbol{x}) \\
[\![\boldsymbol{u}]\!] &= \boldsymbol{u}\,|_{\boldsymbol{x} \in \partial\Omega^+ \cap \Gamma} - \boldsymbol{u}\,|_{\boldsymbol{x} \in \partial\Omega^- \cap \Gamma} \;.
\end{aligned}
\tag{1}
$$

The function $M_\Gamma(\boldsymbol{x})$ consists of the HEAVISIDE-function $H_\Gamma(\boldsymbol{x})$ placed on the discontinuity line $\Gamma$ ($H_\Gamma(\boldsymbol{x}) = 1 \,\forall \boldsymbol{x} \in \Omega^+$ and $H_\Gamma(\boldsymbol{x}) = 0 \,\forall \boldsymbol{x} \in \Omega^-$) and a smooth function $\varphi(\boldsymbol{x})$

$$
M_\Gamma(\boldsymbol{x}) = H_\Gamma(\boldsymbol{x}) - \varphi(\boldsymbol{x}), \quad \forall \boldsymbol{x} \in \Omega
\tag{2}
$$

restricting the effect of the displacement jump to the vicinity of the localization line.

### 2.2 *The strong discontinuity approach*

Using the kinematics defined by (1) a two-field BVP may be formulated with the regular displacement field and displacement jumps as primary unknowns. Different approaches to this BVP have been adopted in the literature (cf. (Samaniego 2003) for a systematic overview): among them the *Strong Discontinuity Approach (SDA)* gained wide popularity.

According to the classification of possible models within the SDA by (Jirásek 2000) the *Statically and Kinematically Optimal Nonsymmetric (SKON)*-approach is used within the present formulation. A simple RANKINE-criterion – suitable for mode-I fracture – is employed for triggering and controlling cracking and the concept of fixed cracks has been adopted. An exponential softening relationship is used. The model accounts for normal and tangential crack opening. The unknown displacement jumps are condensed at element level (Feist & Hofstetter 2003) by a multi-surface return-mapping algorithm (Simo & Hughes 1998). To this end the traction-continuity condition is enforced along the localization line (Oliver 1996b) at element level.

Instead of describing the particular model in detail the problem of placing and aligning the discontinuity segments at element level will be dealt with.

## 3 REPRESENTATION OF DISCONTINUITIES

In the model briefly outlined in the previous section some discontinuity-line $\Gamma$ is approximated by line-segments placed in the elements crossed by the respective discontinuity. Thus, for each of those elements information both on the direction of the line-segment and its position is required.

As far as the direction is concerned the information obtained from the (local) constitutive model may be exploited. Thus, in case of the employed RANKINE-model the direction is given by the principal stress exceeding the tensile strength. Since the concept of fixed cracks is used the normal vector $\boldsymbol{n}$ remains fixed throughout further loading.

The position of the discontinuity within a particular element may be determined individually for each element as an initial attempt. As the present model is based on a simple linear triangular element with a constant strain-field and constitutive response, the discontinuity-segment could be placed at an arbitrary point of the element. A suitable choice would be to select the centroid of an element. However, in this case discontinuity-segments of neighboring elements will be discontinuous across their common edges. Consequently, the actually continuous discontinuity-line is only poorly captured: A particular node shared by several elements may be found at the same time in $\Omega^+$ and $\Omega^-$ for different elements. However, an advantage of this strategy is its local character (with respect to the element level).

The problem of placing discontinuities is empirically investigated by means of numerical simulations of the wedge-splitting-test conducted by (Trunk 2000). The square-shaped specimen has a vertical notch with a length of about half of the specimen height. It is supported below the center of gravity of each half of the specimen (Fig. 1a). The horizontal test load is applied by a vertically pushed wedge on the upper lateral faces of the notch. The load-displacement diagram can be found in Fig. 1c (curve a). Numerical simulations are carried out employing an unstructured triangular mesh (Fig. 1b), which is intentionally not aligned with the vertical macroscopic crack of the real specimen.

By applying the SDA-model with placing the discontinuities individually within each element, the load-displacement curve denoted by (b) in Fig. 1c is obtained, which strongly deviates from the experimental one. The reason for this is revealed by Fig. 2a showing the elements enriched by a displacement jump at the end of the analysis: A large number of elements covering an ample area of the specimen is found to be affected. This behavior originates in a poor resolution of the macroscopic crack direction by using the local direction of the maximum princi-

pal stress. This becomes obvious when scrutinizing the situation during the very first load-steps of the analysis in a close-up of the center of the specimen (Fig. 2d): The crack emerges from the center element in a perfect vertical direction. However, the crack-directions in the two neighboring elements, which start to crack in the next two load-steps, deviate considerably from the vertical direction. As cracks remain fixed upon further loading severe stress-locking occurs. This leads to spurious cracking in neighboring elements shown by the subsequent load-steps in Fig. 2d.

Next, the same model is employed, however, with the direction of the crack-segments in the individual elements not determined from the local principal stress tensor but artificially prescribed in vertical direction. In this case a load-displacement curve exhibiting at least some peak-load and softening branch is obtained (Fig. 1c, curve c), although the load-carrying capacity of the specimen is largely overestimated. Obviously, stress locking phenomena are present also in this formulation. A closer look at the elements enriched by a displacement jump in Fig. 2b shows that the cracked elements are located in a narrower band slightly offset to the right of the vertical axis of symmetry. However, even worse than in the former case, the crack also reaches the top of the specimen. The three initial stages of cracking in Fig. 2e offer a rather optimistic situation. However, as the fourth element starts cracking, the crack is offset to the left. Thus, the crack in element 4 does not intersect the common edge with element 3 but induces further cracking to its upper-left neighbor-element. This obviously leads again to spurious cracking and an unrealistic behavior.

Instead of placing discontinuities individually in each element yielding a discontinuous approximation of the crack-path, the crack (still prescribed to be exactly vertical) is now forced to be continuous across element-edges. The load-displacement curve is resolved very realistically by this manipulation (Fig. 1c, curve d). The cracks are restricted to a vertical band of elements shown in Fig. 2c. As the close-up of the initial load-steps in Fig. 2f shows, the continuous crack-path ensures that common edges of adjacent elements are correctly intersected by the crack-segments avoiding spurious cracking and load-transfer.

Summarizing the observations it appears to be necessary to enforce continuity of cracks across element-edges. This appears to be more realistic in the physical sense when dealing with macroscopic cracks. A more formal explanation can be found in (Samaniego 2003). On the other hand the determination of the crack-direction seems to need some improvement in order to make the artificial prescription of the crack direction, chosen in this test, dispensable. These observations are in full accordance to similar considerations by (Jirásek & Zimmermann 2001).
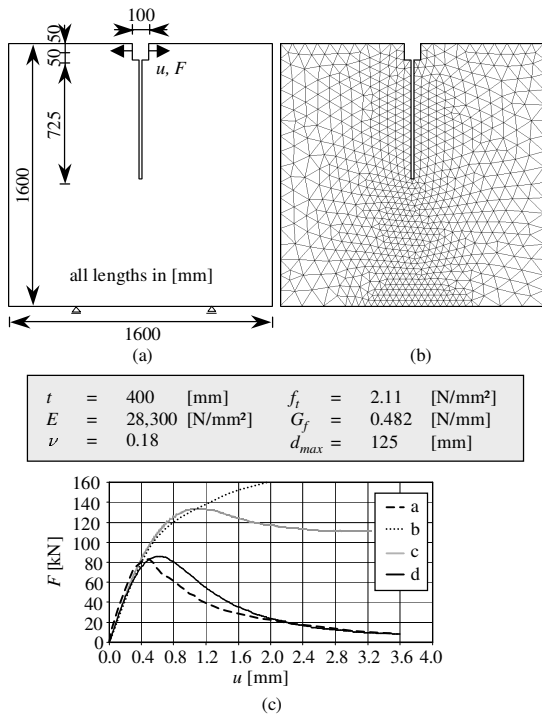


Figure 1. Numerical investigation of a wedge-splitting-test: (a) geometry, loading and material parameters of specimen, (b) finite element mesh and (c) load displacement curves
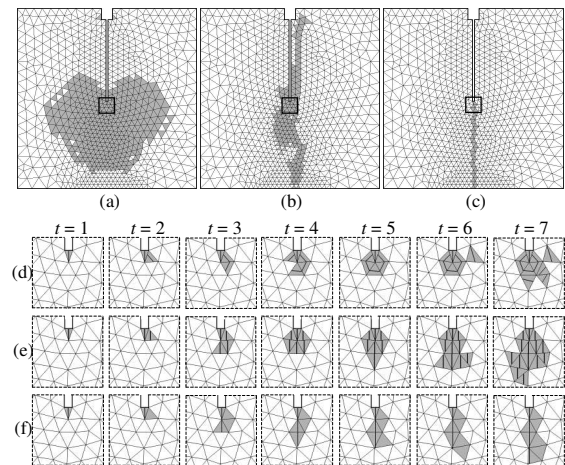


Figure 2. Elements exhibiting a displacement jump (shaded grey) and close-ups of the initial load-steps for: (a), (d) discontinuous crack-path based on local principal stress direction, (b), (e) discontinuous crack-path with prescribed crack direction, (c), (f) continuous crack-path with prescribed crack direction.

## 4  CRACK-PATH CONTINUITY

In the following the enforcement of a continuous crack-path will be addressed. In general, this requires the exchange of information of adjacent elements concerning the crack position. Consequently, the local character of the SDA-model is lost. Algorithms dedicated to the identification of material points along which the discontinuity proceeds can be termed as *tracking algorithms* (Oliver et al. 2002).

### 4.1  *Tracking algorithms*

A traditional way of tracking discontinuities is a *local tracking strategy* (Oliver et al. 2002): The propagation of a discontinuity is traced by geometric calculations starting from its *root element*, i.e. the element from which the discontinuity emanated. If within an element cracking is indicated either an already existing crack is propagating through the respective element or a new crack emerges in the respective element. In the former case the position of the discontinuity-segment is obtained from the geometric information of the discontinuity-path. In the latter case the element becomes a new *root-element* for which it is a suitable choice to place the discontinuity-line at the centroid of the element. This algorithm requires information on the element-connectivity and nodal coordinates.

In contrast to this intuitive algorithm (Oliver et al. 2002) proposed a *global tracking algorithm*: Its basic idea is to trace at once all possible discontinuity paths at some time $t_n$: Consider a vector field $\boldsymbol{N}_n(\boldsymbol{x})$ describing the potential discontinuity-normals at any point $\boldsymbol{x}$ in the domain $\Omega$. For 2D-problems the vector field $\boldsymbol{T}_n(\boldsymbol{x})$ fulfilling the condition $\boldsymbol{T}_n(\boldsymbol{x}) \cdot \boldsymbol{N}_n(\boldsymbol{x}) = 0$ represents the tangents to the potential discontinuity-lines and thus provides information on the potential direction of its propagation. Constructing a scalar field $\theta_n(\boldsymbol{x})$ with isolines representing envelopes to the vector field $\boldsymbol{T}_n(\boldsymbol{x})$ implicitly supplies all possible discontinuity-lines. The scalar field $\theta_n(\boldsymbol{x})$ can be obtained as the solution of a BVP in the domain $\Omega$ which resembles a stationary heat conduction problem with an orthotropic heat conductivity matrix (Oliver et al. 2002). The axes of orthotropy are thereby defined by the vector fields $\boldsymbol{N}_n(\boldsymbol{x})$ and $\boldsymbol{T}_n(\boldsymbol{x})$. Thus, each existing discontinuity-line $\Gamma_i$ can be characterized by a constant scalar value $\theta_{\Gamma_i}$. For elements indicating incipient cracking it has to be checked, if one of the isolines of the scalar field $\theta_{\Gamma_i}$ – each corresponding to a specific discontinuity-line $\Gamma_i$ – crosses the element domain. If so, the position of the discontinuity $\Gamma_i$ is defined by the locus of the respective isoline $\theta_{\Gamma_i}$ within the element. Otherwise, the element is viewed as a new root element defining a discontinuity-line $\Gamma_j$. The scalar value $\theta_{\Gamma_j}$ corresponding to this new discontinuity is obtained by interpolating the scalar value at the root-element centroid from the nodal values. According to the fixed crack concept the axes of orthotropy remain fixed once the element is cracked, whereas these axes in general rotate upon further loading in uncracked elements.

In a finite element setting the global tracking algorithm may be formulated as an uncoupled two-field BVP consisting of the mechanical and the pseudo-heat conductivity problem. In contrast to the local tracking algorithm no information on the mesh-data is required for crack-tracking, although on the other hand the number of total degrees of freedom is increased by the pseudo heat conductivity problem.

A detailed investigation of the approach proposed by (Oliver et al. 2002) reveals, that the isolines of the scalar field $\theta_n(\boldsymbol{x})$ obtained by the proposed algorithm in general only provide approximations to the envelopes for the vector field $\boldsymbol{T}_n(\boldsymbol{x})$. The approximative nature of the computed envelopes is a consequence of the finite number of sampling points. Spurious rotations of the isolines of the scalar field emerge from this fact leading to slightly changing representations of the discontinuity line. The topic is covered in more detail in (Feist & Hofstetter 2003).

### 4.2  *Partial domain tracking algorithm*

Certain drawbacks of the described tracking algorithms can be circumvented by the proposed *partial domain tracking algorithm*: The basic idea of interpolating the position of discontinuities by means of the isolines of some scalar field is maintained from the *global tracking algorithm*. However, the spurious rotations of the isolines in elements with existing cracks is avoided by constructing the scalar field only for a set of those elements which are already crossed or potentially will be crossed by discontinuity-lines.

Consider the following situation at time $t_n$ with an already existing root-element $r_i$ and a set of elements crossed by the discontinuity line $\Gamma_i$. At time $t_n$ the potential continuation of the discontinuity line $\Gamma_i$ for time-step $\Delta t_{n+1}$ shall be predicted. The discontinuity line $\Gamma_i$ will be represented by the isoline $\theta_{\Gamma_i}$ of a scalar field $\theta(\boldsymbol{x})$ passing through the center of the root element. At first, the scalar field in a given root element $r_i$ is determined. As the isolines of the scalar field have to be parallel to the direction-vector of crack-propagation $\boldsymbol{t}^{(e)}$, for the gradient of the scalar field to be constructed in element $e$ it must hold

$$\frac{\partial \theta^{(e)}}{\partial \boldsymbol{x}} = c \cdot \boldsymbol{n}^{(e)}, \quad c \in \mathbb{R}. \tag{3}$$

As long as $c \neq 0$ is fulfilled, an arbitrary number may be assigned to $c$, as it does not influence the orientation of the isolines. As an additional information for constructing the scalar field an arbitrary scalar value at some point (e.g. centroid) within the element domain is prescribed. The scalar field may now be determined at the element nodes. Providing the information of a particular scalar value and the gradient of the field resembles the idea of prescribing fictitious nodal scalar values within the global tracking algorithm (Oliver et al. 2002).

The discontinuity path is then traced over elements connected to the root-element and sharing the same scalar value $\theta_{\Gamma_i}$ by extending the scalar field to the domains of such elements. To this end $\boldsymbol{n}^{(e)}$ provides the information on the gradient of the scalar field. The procedure is repeated until the boundary of the mesh is reached.

Once the scalar field is constructed for all subdomains of the mesh (each corresponding to a particular discontinuity-line), it can be exploited for crack-prediction purposes in the following time-step. The algorithm then exactly follows the ideas of the one proposed by (Oliver et al. 2002). For a comprehensive description of the algorithm see (Feist & Hofstetter 2003) and (Feist 2004).

The proposed algorithm requires storage of nodal coordinates and the element connectivity (essentially equal to the *local tracking algorithm*). However, it does not require to solve a BVP in order to determine the scalar field $\theta$ (as for the *global tracking algorithm*). The scalar field is rather calculated after each time-step only for those nodes connected to elements crossed by the (potential) discontinuity. As the algorithm proceeds from element to element there is no need to solve a large system of equations. Thus, the algorithm combines the advantages of the *local* and the *global tracking algorithm*.

## 5 COMPUTATION OF CRACK DIRECTION

The second important ingredient for a realistic representation of crack-paths is the determination of the direction the cracks will proceed. Instead of obtaining this information from the local constitutive model it is proposed to use the principal direction of the (smooth) nonlocal strain tensor (Feist & Hofstetter 2003). To this end a nonlocal averaging operator based on a bell-shaped weighting function is employed.

## 6 NUMERICAL EXAMPLES

The model constructed step-by-step in the preceding sections is investigated in its full format on the ba-



deformation scale factor: 50
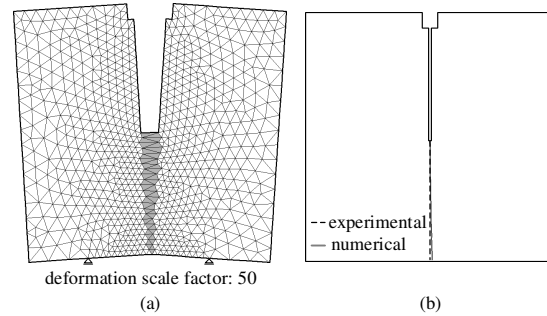
(a)                                        (b)

Figure 3. Results of numerical investigation of the wedge-splitting-test: (a) deformed specimen and (b) crack-pattern.

sis of numerical simulations of benchmark problems. The latter are documented in the web-based platform of the thematic network *NW-IALAD* (Ialad 2003) dedicated to the *Integrity Assessment of Large Concrete Dams* and funded by the EU. The core of the network is an internet platform (Ialad 2003) serving as a forum for present members and open to new participants. Corresponding to the different work-packages and task-groups it offers databases, reviews of dam performance, dam maintenance, repair and rehabilitation, safety assessment and dam calculations. In the context of the latter systematic comparisons of classic and enhanced numerical models for the simulation of the structural behavior of concrete dams will be provided. To this end documentations of benchmark problems are offered for participants willing to provide numerical simulations based on particular models for evaluation purposes.

### 6.1 Wedge-splitting test

The numerical simulation of the wedge-splitting-test (Trunk 2000) (Fig. 1a) already presented in the context of the outline of evolution of the present SDA-model is described first. The interaction-radius $R$ required for the nonlocal averaging of the strains is taken as 2.5-times the maximum aggregate size of $d_{max} = 125$ mm. Fig. 3a presents the deformed specimen with displacements magnified by a factor of 50. The computed crack-path shown in Fig. 3b representing an astonishingly straight image of the real crack-path shows the insensitivity of the model with respect to mesh-bias effects. Finer discretizations of the model yield exactly the same results proving objectivity (not shown in this work, refer to (Ialad 2003)).

### 6.2 Mixed-mode fracture test

The second example investigated with the proposed model is a mixed mode fracture test taken from the
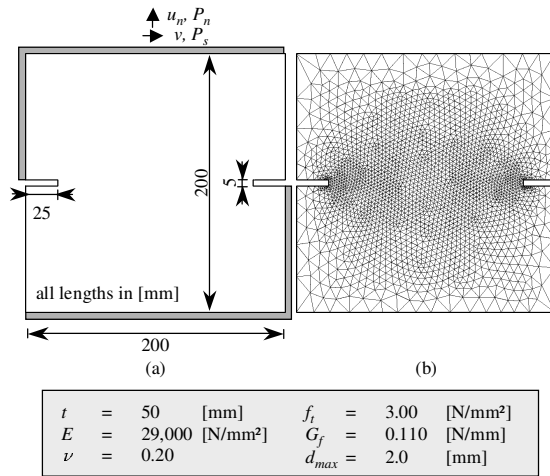
Figure 4. Numerical investigation of a mixed-mode-fracture test: (a) geometry, dimensions, loading and material parameters of test-specimen, (b) employed finite-element mesh.

thesis of (Nooru-Mohamed 1992). The specimen (Fig. 4a) consists of a quadratic panel with horizontal notches located at mid-length of the vertical faces. The specimens were subjected to a combination of shear and tension forces for various load-paths. During load-path 4(c) first a pure shear load was applied up to the maximum sustainable shear-force $P_s = 27.5$ kN followed by tensile loading with the shear-force kept constant. The experimentally observed crack-pattern consists of two strongly curved cracks propagating from the notches. Hence, these tests offer an excellent opportunity to examine the capabilities of the proposed model to tackle multiple cracks and curved crack-paths.

The mesh used for the numerical simulations is depicted in Fig. 4b. As can be seen from the deformed mesh in Fig. 5a the elements with a displacement jump are found on two separate curved paths through the entire mesh. Fig. 5b depicts the discrete crack-paths each enclosing an angle of app. 90° between the tangents at the beginning and at the end of the cracks. When compared to the plots of the experimentally obtained crack-paths perfect resolution of the macroscopic cracks by the numerical simulation is revealed. Results of simulations of other load-paths are documented in (Ialad 2003) also showing good agreement with the experiments.

### 6.3 Koyna dam

As an example for a large-scale analysis a numerical simulation of the well known Koyna dam is presented. The dam was struck by a short duration earthquake in 1967, which caused severe damage to the dam. The dam is a 850 m long concrete gravity dam with a crest height of 103 m (Fig. 6a). At a level of 66.5 m (all levels related to base level) the downstream face has a characteristic bend. The upstream face is slightly inclined by 24:1. At the time of the earthquake the reservoir level was at 91.75 m. In (Chopra & Chakrabarti 1973) horizontal cracks at the upstream face of some blocks at levels ranging between 60 and 66 m are reported. On the downstream face cracks were also found in the vicinity of the bend at levels around 66 m.

The damage of the dam had been thoroughly investigated by many researchers using very different constitutive approaches. Although the dam is rather heterogeneous with respect to the used concrete mix design, quite similar and homogeneous material parameters were used (Lee & Fenves 1998). The parameters employed in the present study are summarized in Fig. 6.

The FE-discretization is based on the geometry and the dimensions given in Fig. 6a. The slightly inclined upstream face is considered vertical. The used FE-mesh is depicted in Fig. 6b. It consists of 8097 SDA-enriched CST elements based on a plane strain formulation and 4180 nodes (8360 dofs). A rather fine and regular discretization is used for the bottom part up to 10 m above ground and for the region between 46.5 and 66.5 m elevation. The remainder of the domain is discretized with an unstructured, coarse mesh. As in many other reported analyses neither the supporting rock nor the interface between rock and concrete, i.e. the contact joint, are discretized. The monolith is considered to stand on a rigid surface. However, to account for the effects of the contact joint cracks may propagate horizontally in the bottom row of elements.

Element sizes in the presumptive fracture areas vary between $0.5 - 0.6$ m providing uniqueness of the results in general. However, for certain unfavorable crack directions with respect to the mesh layout stability may be lost anyhow. Therefore, in order


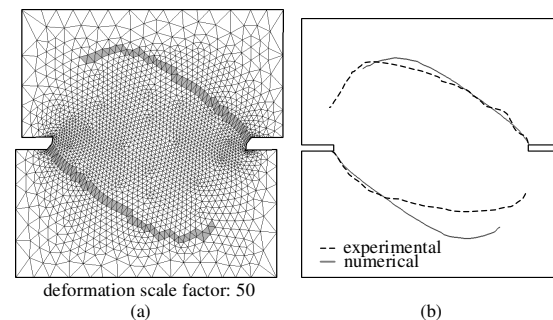
deformation scale factor: 50

(a)          (b)

Figure 5. Results of numerical investigation of a mixed-mode-fracture test: (a) deformed specimen (elements enriched by displacement-jump are shaded grey), (b) calculated crack-pattern.

to increase robustness of the numerical procedure some artificial viscous damping is added (Samaniego 2003).

The dam is initially subjected to dead load followed by the application of hydrostatic water pressure to the upstream face according to a reservoir fill of $h_n = 91.75$ m (Fig. 6c). In the next load step the reservoir level is successively increased up to the height of the dam crest $h_f = 103$ m (Fig. 6d). In the fourth load step the reservoir level is fictitiously raised up to the level that leads to collapse of the dam (Fig. 6e). This level is often termed as the level of *imminent failure flood* $h_{iff}$. It is noteworthy that the aforementioned procedure does not account for a realistic overflow of the dam. (Consequently, hydrostatic pressure is neither acting on the horizontal plane of the dam crest nor on the downstream face.) Sometimes the load-carrying capacity and the safety of a dam against failure are evaluated in terms of the maximum overtopping coefficient $\gamma_{iff} = h_{iff}/h_f$.

The load displacement curve in terms of the over-topping coefficient is shown in Fig. 7a for the range of $\gamma = 0.89 - \gamma_{iff}$ with horizontal displacements related to the unloaded condition of the dam. Obviously, considerable nonlinearity commences already at $\gamma = 1.0$ corresponding to a full reservoir (point (1.00) in Fig. 7a). In fact, when taking a look at the crack pattern in Fig. 7b, a crack at the interface layer at the base of the dam can be detected. This crack already emerges at a reservoir level of app. 95 m. At $\gamma = 1.28$ ($h \approx 132$ m) a marked bend is found in the load displacement curve (point (1.28) in Fig. 7a): A second crack forms at the upstream face (Fig. 7c) at an elevation of 61 m, which is in good agreement with the cracks reported by (Chopra & Chakrabarti 1973). This second crack forms independently of the first one at the most critical section of the cantilever subjected to hydrostatic loading.

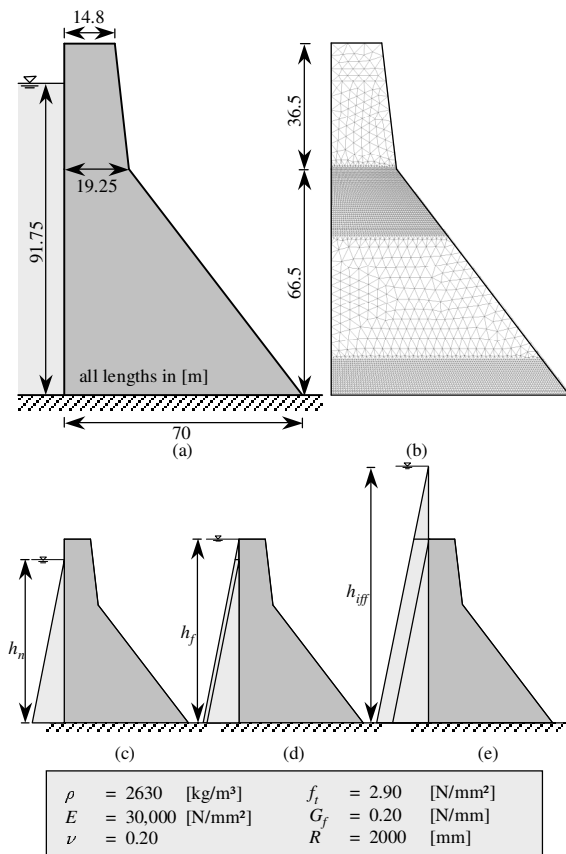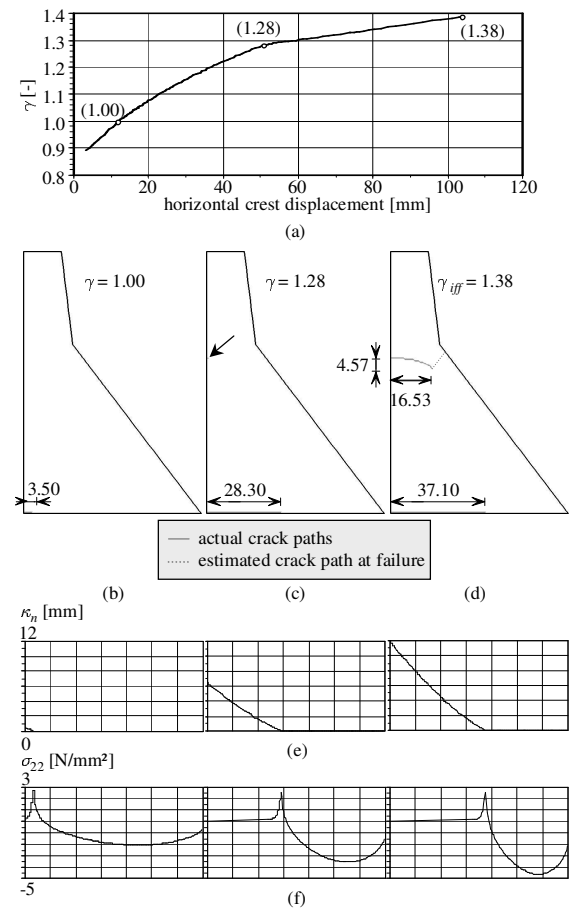Successive loading causes further propagation of



Figure 6. Numerical investigation of the Koyna dam: (a) geometry and dimensions of the dam, (b) employed finite-element mesh and loading due to (c) normal reservoir fill, (d) full reservoir fill, (e) up to imminent failure flood.



Figure 7. Results from numerical investigation of the Koyna dam: (a) overtopping coefficient vs. horizontal dam crest displacement; crack-patterns at (b) full reservoir load, (c) emerging secondary crack and (d) imminent failure flood; (e) crack-opening and (f) vertical stresses along contact joint.

both cracks. The upper crack, starting to propagate horizontally, soon extends downward to the downstream base with an increasing curvature (Fig. 7d). As the crack direction becomes parallel to the downstream face of the dam the crack ceases to propagate. However, as a consequence of the redistribution of loads a third crack emerges exactly from the crack tip of the second crack in a direction perpendicular to the one of the second crack. This situation is encountered at $\gamma = 1.38$ ($h \approx 142$ m). In fact, the structure is already too weak to sustain further load increments and therefore this level is considered as the one of imminent failure flood. Consequently, the dotted curve in Fig. 7d only provides an estimate of the propagation of the third crack. The crack pattern of the second crack is in perfect agreement with the one reported by (Jirásek 1999). However, in (Jirásek 1999) the bottom crack at the interface layer seems to have been neglected.

The diagrams in Fig. 7e, f reflect the crack-opening and vertical stress distribution found along the contact joint at the respective load levels. A maximum crack opening of app. 12 mm is observed at $\gamma_{iff} = 1.38$ with vertical stresses asymptotically tending to zero at the widely open crack. Such widely open cracks would certainly let water of the reservoir penetrate into the opening crack. Due to the high pressure water penetration would become an additional driving force for crack-propagation. Thus, it is questionable if a model without consideration of fluid pressures acting on crack-faces yields reliable results in the particular case. Consideration of fluid penetration into open cracks is covered in a detailed report on the Koyna-dam analysis in (Ialad 2003).

## 7 CONCLUDING REMARKS

A numerical model for the representation of discontinuities in the displacement field was investigated. The model utilizes the concept of the elements with embedded discontinuities and is formulated as a nonsymmetric SDA-model. Shortcomings of the basic model were outlined: Discontinuous resolution of the crack-path appeared as a source of severe mesh-sensitivity and locking effects. To overcome this deficiency it proved to be necessary to enforce continuity of the crack-path, although the simplicity of the basic model is lost. Tracking algorithms provide the essential information to establish crack-path continuity. Existing algorithms were shortly discussed. A new *partial domain tracking* algorithm was presented combining the strong points of the established algorithms.

Objective prediction of the crack-direction was dealt with subsequently: A criterion derived from local constitutive response appeared to be insufficient. A nonlocal averaging procedure was proposed to resolve objective crack-paths.

The improved model was then applied to the simulation of two laboratory tests and a large-scale problem demonstrating the capability of the model and the sketched algorithms.

## REFERENCES

Chopra, A.K. & Chakrabarti, P. 1973. The Koyna earthquake and damage to Koyna dam. *Bulletin of the Seismological Society of America* 63: 381-397, 1973.

Feist, C. 2004. *Numerical Simulations of Localization Effects in Plain Concrete*. PhD thesis, Universität Innsbruck, in prep., 2004.

Feist, C. & Hofstetter, G. 2003. Mesh-insensitive strong discontinuity approach for fracture simulations of concrete. *Proc.Numerical Methods in Continuum Mechanics, NMCM 2003*, Slovak Republic, 2003. CD-Rom.

Ialad 2003. *NW-Ialad Integrity Assessment of Large Dams*, 2003. http://nw-ialad.uibk.ac.at/Wp2/Tg2.

Jirásek, M. 1999. Computational aspects of nonlocal models. *Proc.European Conference on Computational Mechanics*, Munich, 1999. CD-Rom.

Jirásek, M. 2000. Comparative study on finite elements with embedded discontinuities. *Computer Methods in Applied Mechanics and Engineering* 188(1-3): 307-330, 2000.

Jirásek, M. & Zimmermann, T. 2001. Embedded crack model: Part II: Combination with smeared cracks. *International Journal for Numerical Methods in Engineering* 50(6): 1291-1305, 2001.

Lee, J. & Fenves, G.L. 1998. A plastic-damage concrete model for earthquake analysis of dams. *Earthquake Engineering and Structural Dynamics* 27(9): 937-956, 1998.

Nooru-Mohamed, M.B. 1992. *Mixed-mode Fracture of Concrete: an Experimental Approach*. PhD thesis, University of Technology, Delft, 1992.

Oliver, J. et al. 2003. A study on finite elements for capturing strong discontinuities. *International Journal for Numerical Methods in Engineering* 56(14): 2135-2161, 2003.

Oliver, J. et al. 2002. On strategies for tracking strong discontinuities in computational failure mechanics. In H.A. Mang, F.G. Rammerstorfer, and J. Eberhardsteiner, (eds), *Proc.World Congress on Computational Mechanics, WCCM V*, Austria, 2002. Vienna University of Technology. http://wccm.tuwien.ac.at.

Oliver, J. 1996a. Modelling strong discontinuities in solid mechanics via strain softening constitutive equations. Part 1: Fundamentals. *International Journal for Numerical Methods in Engineering* 39(21): 3575-3600, 1996.

Oliver, J. 1996b. Modelling strong discontinuities in solid mechanics via strain softening constitutive equations. Part 2: Numerical simulation. *International Journal for Numerical Methods in Engineering* 39(21): 3601-3623, 1996.

Samaniego, E. 2003. *Contributions to the Continuum Modelling of Strong Discontinuities in Two-dimensional Solids*. PhD thesis, UPC Barcelona, 2003.

Simo, J.C. & Hughes, T.J.R. 1998. *Computational Inelasticity*, volume 7. Springer, New York, 1998.

Trunk, B. 2000. *Einfluss der Bauteilgrösse auf die Bruchenergie von Beton*. Aedificatio Publishers, Freiburg, 2000. in German.